Opto-electronic pattern recognition system

H. J. TIZIANI, B. H. BEYELER & W. WITZ

Institut fur Technische Physik, ETH-Aussenstation, Hönggerberg, Zurich

An opto-electronic technique for the classification of grains of photo-
graphic emulsions by shape is described. Fortunately, the shapes to be
distinguished differ only in their two-dimensional rotational symmetry
group. A special optical filtering procedure has been developed to take
account of the implied positional and rotational invariance. The transfer
from the optical to the electrical signal is obtained in a simple manner.
The method works satisfactorily even for a rather complicated cluster.
Some results are discussed.

OBJECTIVE CRITERIA for the quality of photographic
emulsions are required. The projection of the indi-
vidual AgBr-crystals of especially prepared emul-
sions are produced by an electron microscope at a
lateral magnification of 10, 000. According to the pre-
cipitation conditions, different shapes of crystals
occur: cubes, octahedrons and triangular or hexagonal
plates. Since the orientation of the crystals is usually
such that one side is parallel to the substrate plane,
the projections of the crystals are square, rhomboidal,
triangular or hexagonal as shown in Fig. 1. This pic-
ture represents a mixture of differently precipitated
emulsions to show all the characteristic shapes of
photographic grains at once. The electron-microscopi-
cal preparation has been performed to obtain the pro-
jected areas of the grains only. The crystals are
sparsely distributed, but some superpositions of two
or occasionally more objects forming clusters can
occur. The range of variation in the object size of the
emulsion to be studied is about 0. 05-0. 5μm.

Manufacturers of photographic emulsions are interes-
ted in the statistics of these crystals in shape and
size. A method to determine these two parameters
automatically must be developed. Measurement of the
crystal size to the accuracy required is not too diffi-
cult. To investigate the statistics of the shapes is not,
however, an easy pattern recognition problem. Posi-
tion and orientation of the crystals are of no impor-
tance and small discrepancies, for instance rounded
corners, should be of no significance. Thus the pat-
tern recognition system to be devised must classify
the shapes which occur, either separately or in clus-
ters, into four groups independently of position or
orientation. Such a system is described here.

POSSIBLE SOLUTIONS

In principle it is possible to scan the pattern shown
in Fig. 1 photoelectrically and to analyse the infor-
mation in a digital computer. This method, however,
needs an exceedingly complicated algorithm.

The reasons for not using the well-known optical
filtering techniques such as those proposed by Vander

Lugt,[1] or Armitage & Lohmann,[2] for coherent and
incoherent illumination respectively are now briefly
discussed. These methods seek correlations between
the presented pattern of the unknown material and
the filter of the standard comparison object. Such
filters are selective with respect to variation of both
size and orientation. In this case classification of the
objects into the four groups only is required. Never-
theless, it would be possible to employ a large num-
ber of rotating filters to account for this size dis-
crepancy. Alternatively, zoom objectives or the
method given by Vander Lugt[3] could also be used.
The methods mentioned have not, however, been found
to be suitable; they are very sensitive to the accuracy
of positioning of the filters and are very slow.

An opto-electronic analogue method was finally adop-
ted with the required invariance properties. The
following sections are devoted to the new method. It
is assumed that the selection of the cluster or single
object is carried out in the object space prior to the
filtering procedure.

Fig. 1 Example of an electron micrograph

OPTO-ELECTRONIC PATTERN RECOGNITION SYSTEM

The two dimensional Fourier transform of the object is obtained in the back focal plane of the lens L shown in Fig. 2. The object in the plane P_1 is illuminated by a plane wave. The spectrum a(x, y) of the object with the complex amplitude A(u, v) obtained in the back focal plane P_2 of the lens L is (ref 4)

$$a(x, y) = \int\limits_{-\infty}^{\infty} \int A(u, v)\exp\left[-2\pi i(ux + vy)\right]dudv$$

u and v are the coordinates in the object plane and x, y are the normalised coordinates in the back focal plane which are related to the geometrical coordinates X, Y in the following way

$$x = -\frac{X}{\lambda f}, \quad y = -\frac{Y}{\lambda f}$$

where λ is the wavelength of the light and f the focal length.

The intensity in the back focal plane is

$$i(x, y) = |a(x, y)|^2$$

and, as is well-known, i(x, y) is invariant on translation of the object in the (u, v) plane.

Typical intensity spectra of examples of each of the four groups are shown in Fig. 3. The rotational symmetry of the corresponding object is manifest in the spectrum. The reason for the three-fold symmetry of the triangular object is explained in the Appendix.

Fig. 3 shows that each of the four groups is distinguished by the azimuth dependence of the energy distribution of the intensity spectrum

$$e(\Phi) = \int\limits_{0}^{\infty} i(x, y)r \, dr \quad \text{with } r = (x^2 + y^2)^{1/2} \qquad 1$$

Except for an energy factor, the function of $e(\Phi)$ is independent of the extent of the object, as indicated in the Appendix. The same conclusions apply with reasonable approximation to the modified function

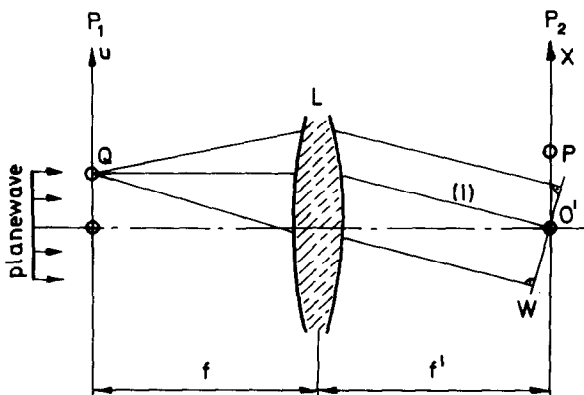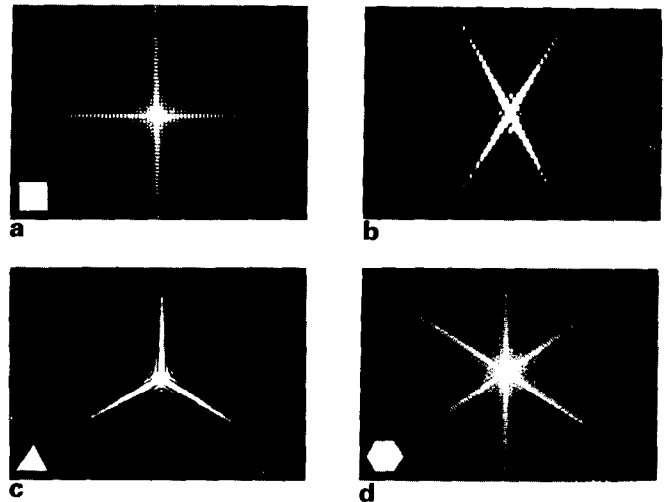$$e'(\Phi) = \int\limits_{r_0}^{r_1} i(x, y)r \, dr \quad \text{with } r_1 \gg r_0$$

Fig. 3 Typical spectra obtained for each of the four object groups: (a) square, (b) rhombus, (c) triangle, (d) hexagon

where $r_0 >$ the extent of the zero order of the spectrum of the smallest object to be investigated. The limits of integration are physically reasonable, since the zero order of the spectrum contributes a constant intensity to $e(\Phi)$. Knowing that the central intensity in the spectrum is proportional to the area of the object, this is used for size determination.

REALISATION OF THE METHOD

The measurement of $e'(\Phi)$ is accomplished by rotating a disc S with its centre on the optical axis and with a transparent sector, as shown in Fig. 4. The light flux is collected by the photo-cathode of a photomultiplier behind the rotating disc. The power of the collected light can be written as

$$f(\Phi) = \int\limits_{\phi - \frac{\Delta\Phi}{2}}^{\phi + \frac{\Delta\Phi}{2}} e'(\Phi) \, d\Phi = e'(\Phi) - \!\!\!*\!\!\!- s(\Phi)$$

where $s(\phi)$ is the characteristic function of the sector slit, $\Delta\phi$ is the angle of the sector, and $-\!\!*\!\!-$ indicates, as customary, the convolution sign. For an appropriately small angle $\Delta\Phi$ ($\Delta\Phi$ of 15° was found to be adequate for the configuration chosen) there is practically no information lost by considering f rather than e'.

The behavior of $f(\Phi)$ as a function of the orientation of the object is obvious. Rotations of the objects correspond to the same rotations in the (x, y) plane and hence a phase shift is introduced. It is useful, therefore, to carry out a one-dimensional Fourier transform of $f(\Phi)$. For this reason it seems appropriate to rotate the diaphragm at constant speed. The frequency was chosen to be $\nu_0 = 80$ cycles and, hence, $\Phi = 2\pi \nu_0 t$.

This produces an electrical signal of the form

$$U(t) = \text{const. } f(2\pi \nu_0 t)$$
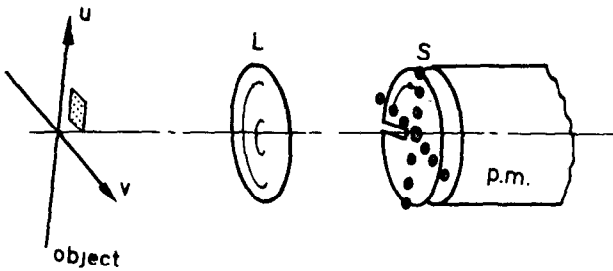
from the photomultiplier.

Fig. 2 Fraunhofer diffraction

Fig. 4 Schematic of the scanning procedure

Its spectrum is

$$u(\nu) = \int_{-\infty}^{\infty} U(t) \exp[-2\pi i\, \nu t]\, dt$$

It is obvious that the time-function $U(t)$ is a periodic function and that therefore only spectra with multiple frequencies of ν_0 are expected. Thus

$$u(\nu) = \sum_{n=-\infty}^{\infty} c_n\, \delta(\nu - n\,\nu_0)$$

A finite integration time introduces a broadening of the spectra, but we are only interested in the ratio of c_n. Because the c_n are the complex Fourier coefficients the moduli of the real function $U(t)$ are related by

$$|c_n| = |c_{-n}| \qquad n = 0, 1, \ldots$$

This is easily verified with the spectrum analyser. A consequence of the rotational symmetry of the objects is the occurrence of coefficients c_n listed in Table 1.

Table 1 Complex Fourier coefficients

group	object	$c_n \neq 0$ for $n =$
k = 2	rhombus	2, 4, 6, 8, 10, 12, ...
k = 3	triangle	3, 6, 9, 12, ...
k = 4	square	4, 8, 12, ...
k = 6	hexagon	6, 12, ...

Fig. 5 shows the time function $U(t)$ as well as the frequency spectrum of a sample of each of the four groups. The arrow indicates the position of $\nu_0(n=1)$. It is easily seen that the modulus $|c_n|$ of the coefficients is invariant to rotation of the object; only a constant phase shift is introduced.

All the desirable invariance properties for the coefficients $|c_n|$ are therefore secured. It remains now to investigate the classification into the appropriate group for a known set of coefficients $|c_n|$. Classification of single objects in the four groups could be achieved according to Fig. 5 and Table 1 by considering only the fundamental frequency of the signal. For analysing clusters, however, a set of coefficients $|c_n|$ must be used.

(i) In an ideal system, the coefficients c_1, c_5, c_7, $c_{11} \ldots$ would not occur. This is, however, not the

case in practice, according to Fig. 5. The reason for the discrepancy is partly due to instrumental error. These coefficients are not carrying useful information and so are neglected in the analysis.

(ii) For $n > 12$ the information content of the coefficients is negligible.

The remaining coefficients which agree with Table 1 are

$$c_2, c_3, c_4, c_6, c_8, c_9, c_{10}, c_{12},$$

This set characterises the pattern in two ways. The length

$$L = \left(\sum |c_n|^2\right)^{1/2}$$

is approximately proportional to the linear dimension of the object (as shown in Appendix) and the direction specifies the shape of the object. From the normalised coefficients $c'_n = |c_n|/L$, four so-called recognition factors $p_k(k = 2, 3, 4$ and 6) may be calculated to obtain an appropriate measure of the group number k. It was found to be adequate to use the linear relation although many other more complicated
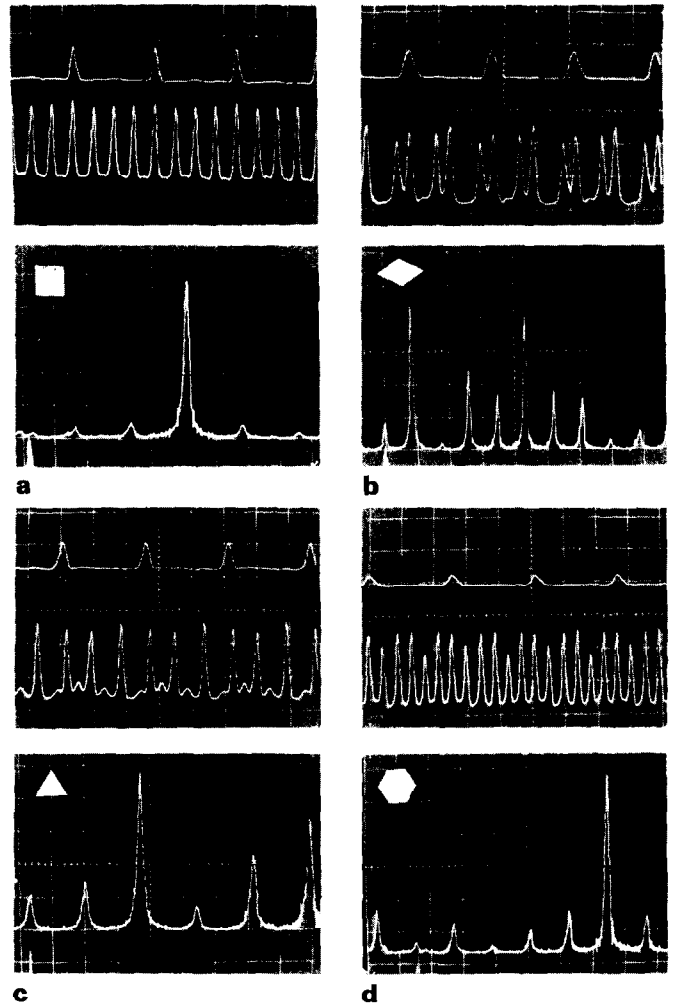

Fig. 5 Typical time functions and the corresponding frequency spectra for a sample of each of the four object groups: (a) square, (b) rhombus, (c) triangle, (d) hexagon
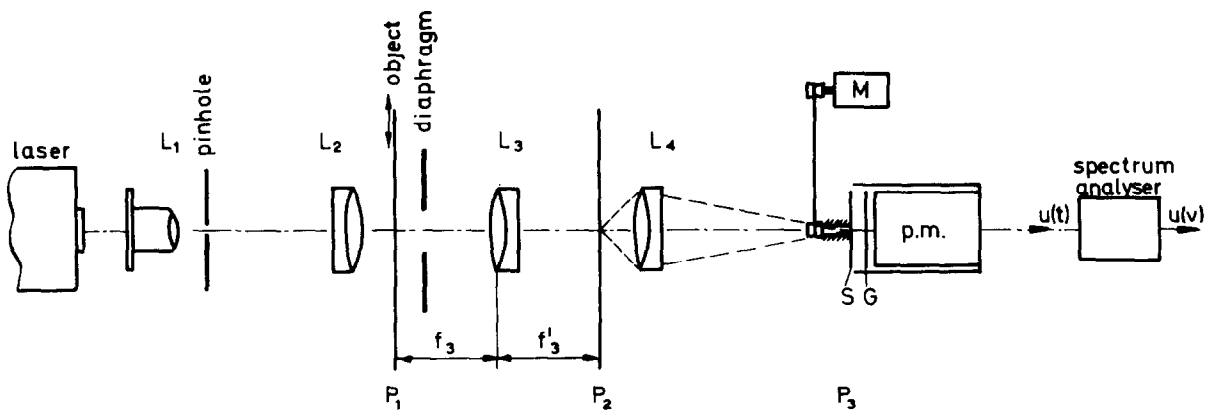
Fig. 6 Schematic of the apparatus

approaches were tried. Hence

$$p_k = \sum_n r_{nk} \, c_n', \quad n = 2, 3, 4, 6, 8, 9, 10, 12$$

The matrix elements r_{nk} were determined empirically and optimised by examining numerous known objects (37), and measuring their coefficients c_n, so that the r_{nk} could be calculated.

The linear transformation in expression 2 may be carried out quite easily using an analogue computer (resistance matrix). A set of appropriately tuned frequency filters may be applied to obtain the coefficients $|c_n|$. At first, these filters were not available, therefore an alternative method of measuring the coefficients on the screen of a spectrum analyser was employed as indicated in Fig. 6.

EXPERIMENTAL PROCEDURE

The apparatus designed for the experimental investigations is shown schematically in Fig. 6, where the laser beam is expanded by the lenses L_1 and L_2. A plane wave of $\lambda = 632.8nm$ illuminates the object in P_1 and the spectrum is formed by lens L_3 in its focal plane P_2. To use a rather short focal length lens L_3 (200mm), an enlarging lens L_4 projects the magnified spectrum onto the photocathode of the photomultiplier through the rotating sector slit S. A frequency-stabilised motor M drives the diaphragm. A ground glass G between the diaphragm and photocathode was useful in eliminating the inhomogeneity of the photocathode. The zero order frequency which is not used for shape determination, can be deviated by a small mirror onto a photodiode for size determination. Typical results obtained with this configuration are shown in Fig. 5.

RESULTS

It should be noticed that for a single and ideal crystal, the recognition factor for the corresponding group is approximately one, but is negligible for the others, provided the normalisation

$$p_k' = \frac{p_k}{[\, \Sigma p^2_k]^{1/2}}$$

is used.

It was found experimentally that out of 42 single objects, including many with considerably rounded corners, the recognition factor of the associated group was >0.7. By contrast the remaining three recognition factors were always <0.4. As has already been pointed out, the determination is unaffected by displacement and rotation of the object.

It remains now to investigate the application of the method to the identification of clusters. The theoretical analysis is complex since a number of non-linearities occur.

(i) Even in the object plane P, superposition is non-linear because the common area of two or more superposed objects has the same unit transmission as the single object.

(ii) Linear superposition of the complex amplitudes of the spatial spectra $a(x, y)$ of two or more objects occurs, but of course, the photomultiplier converts only intensities.

(iii) The coefficients $|c_n|$ are not linear functions of the signal $U(t)$, but depend on the relative phases of the components.

These arguments do not support the linear superposition of the components suggested in expression 2. Nevertheless, further detailed study of the problem has shown that in many cases recognition of compound objects, using the method described above leads to satisfactory results. An analysis of 53 clusters
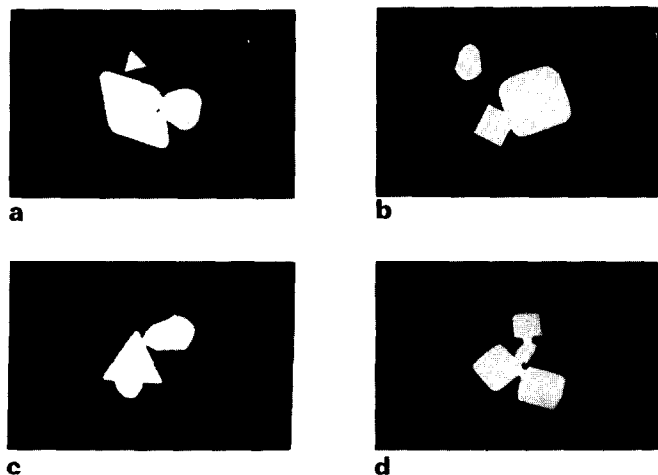

Fig. 7 Representative samples of clusters

has been carried out. Representative samples which were recognized are shown in Fig. 7. The dominant recognition factor was unequivocal in 41 cases and the dominant objects were clearly detected. Only 12 samples were doubtful, giving either no unequivocal identification or leading to wrong conclusion.

CONCLUSIONS

The work presented leads to an automatic pattern recognition system, which may, however, only be applied to specific geometrical objects differing only in their two-dimensional rotational symmetry group such as the crystals described. The desired invariance properties are implicit in the method without the special precautions necessary for the classical filtering methods. Furthermore, the method is fast— which is an important feature. The reliability for single objects was found to be almost 100% and, for clusters, more than 75%.

REFERENCES

1 Vander Lugt, A. A review of optical data processing techniques. Optica Acta, vol. 1. 1968. pp. 1-33.

2 Armitage, J. D. & Lohmann, A. W. Character recognition by incoherent spatial filtering. Appl. Opt. vol. 4. 1965. pp. 461-67.

3 Vander Lugt, A. Operational notation for the analysis and synthesis of optical data-processing systems. Proc. IEEE. vol. 8. 1966. pp. 1055-63.

4 Born, M. & Wolf, E. Principles of optics. 1965.

5 Hannes, H. Interferometrische Messungen an Phasenstrukturen fur die Holographie. Optik. vol. 26. 1967. pp. 363-80.

APPENDIX

Symmetry of the spectrum of the triangle In general, the Fourier transform of a real function $A(u, v)$ is

$$FT[A(u, v)] = a(x, y) = a^*(-x, -y)$$
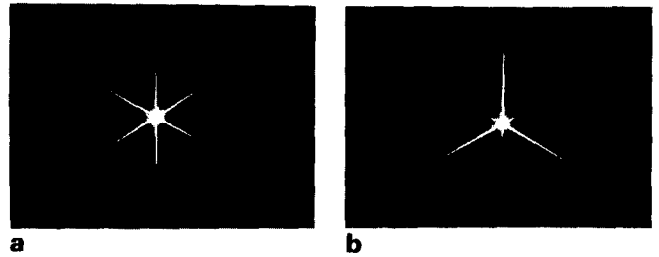
and $|a(x, y)|^2 = i(x, y) = i(-x, -y)$ 3

Fig. 8 Spectra of triangles with and without induced phase modulation:

(a) is spectrum of a triangle punched into metal foil showing six-fold symmetry

(b) is a triangle copied on typolith showing threefold symmetry

The intensity spectrum of a real function is always symmetrical as shown in Eqn 3. Hence, the spectrum of a real triangle has the sixfold symmetry shown in Fig. 8a. A triangle punched into a disc was used as object. By contrast, in Fig. 8b, the transparency of the object, a photographic film (typolith), is no longer real. It can be shown that a phase change due principally to a surface swelling near the edge of the transparency object caused a phase modulation of the light and, hence, leads to a threefold symmetry of the spectrum as shown in Fig. 3 and 8b. The width of the emulsion swelling was found to be about 50μm for objects of 0.5-5.0mm, and an increase of the thickness of about 300nm occurred[5]. This investigation will be subject of a further publication.

Size invariance of the function e(Φ) From $A(u, v) \xrightarrow{FT} a(x, y)$ it follows that

$$\bar{A}(u, v) = A(cu, cv) \xrightarrow{FT} \bar{a}(x, y) = c^{-2} a\left(\frac{x}{c}, \frac{y}{c}\right).$$

Substitution in Eqn 1 gives

$$\bar{e}(\Phi) = e(\Phi) \cdot c^{-2}$$

Changing the upper limit of integration from ∞ to $r_1 \gg r_0$ does not appreciably change $e(\Phi)$ for as $r \to \infty$, $|a(x, y)|^2 \approx 0[1/r^2]$. By contrast, however, the lower limit of integration r_0 reduces the low frequency content of $e(\Phi)$ which is, of course, more important for larger objects (small zero order spectrum). The suppression of the low frequencies is largely compensated by the increase of intensity in the spectrum due to the larger object.